


Thermal analysis study of solid dispersions hydrochlorothiazide

Cinthy Maria Pereira de Souza^{1,2}  · Jonh Anderson Borges dos Santos² ·
Agnaldo Luiz do Nascimento² · José Venâncio Chaves Júnior² ·
Fernando José de Lima Ramos Júnior^{1,2} · Severino Antônio de Lima Neto² ·
Fábio Santos de Souza^{1,2} · Rui Oliveira Macêdo^{1,2}

Received: 21 May 2016 / Accepted: 7 January 2017 / Published online: 27 January 2017
© Akadémiai Kiadó, Budapest, Hungary 2017

Abstract Solid dispersions (SD) are used as a technological strategy to increase the aqueous dissolution rate of poorly soluble active pharmaceutical ingredients, such as hydrochlorothiazide (HCTZ), an antihypertensive used frequently in medical clinics. The aim of this study was to characterize solid dispersions of HCTZ obtained with different processing adjuvants, using the DSC, TG, XRPD, FTIR and SEM techniques, and to evaluate the influence of carriers used in biopharmaceutical performance by analyzing dissolution efficiency. The SDs were obtained using the solvent method, and *spray drying* was used as the drying technique. The carriers used PEG 1500, sodium lauryl sulfate and PVP K30. The calorimetric analysis and XRPD showed amorphous behavior to SDs that used hydrophilic polymer as a carrier, and thermogravimetric analysis showed maintaining thermal stability of the HCTZ for most dispersions. FTIR detected intermolecular interactions of hydrogen bonds, while SEM showed the formation of microparticles with a tendency to sphericity. Acquired morphology associated with amorphization contributed to the increase in dissolution efficiency of dispersions, being that this SD (HCTZ/PVP K30) showed the best increase in dissolution. We therefore concluded that the analytical techniques used were of fundamental importance to the characterization of pharmaceutical

products developed as to their physicochemical properties and the presence of the oral bioavailability of HCTZ.

Keywords Thermal analysis · FTIR · XRPD · Dissolution efficiency · Hydrochlorothiazide

Introduction

Among the strategies proposed to circumvent the low aqueous solubility of APIs, there are solid dispersions (SDs), which are pharmaceutical forms obtained by different technological processes and consist of dispersing a pharmacologically active component into a matrix biologically inert (i.e., a carrier) [1, 2]. This technique produces advantages such as a significant reduction in API particle size, possibly at the molecular level, increased wettability and porosity, increased uniformity and surface contact and, in general, a change from crystalline state to an amorphous state. As a result, this technique provides higher rates of dissolution and better solubility, which improves the therapeutic action due to increased bioavailability [3–5].

Polymers or combinations of polymers and surfactants have been proposed in an attempt to adapt the physicochemical properties of the polymers to the solid dispersion system and increase its stability [6]. Commonly reported excipients used in the preparation of solid dispersion include propylene glycol (PG), polyethylene glycol (PEG) 4000, 6000 and 8000, Tween—80, and povidone (PVPK-30) [7].

The main methods used to obtain dispersed system are: melting, solvent and fusion-solvent [4]. In the solvent method, the drug and the carrier are solubilized in a common organic solvent, which is evaporated under constant stirring, producing a dry residue and solid [8]. This method has been

✉ Cinthy Maria Pereira de Souza
cinthyampsouza@hotmail.com

¹ Department of Pharmaceutical Sciences, Postgraduate Program in Pharmaceutical Sciences, Federal University of Pernambuco, University City, Recife, PE, Brazil

² Department of Pharmaceutical Sciences, Unified Laboratories of Pharmaceutical Development and Assays, Federal University of Paraíba, CEP 58051-970, Castelo Branco, João Pessoa, PB, Brazil

preferred because it prevents the thermal decomposition of the API or vehicles, since it requires relatively low temperatures for evaporating the solvent [9, 10]. Solvent removal may be performed by different techniques; among them, the following stand out: rotary evaporation, spray drying and freeze drying. The spray drying produces SD of particles with reduced size, low solvent residue in the systems, changes in the crystallinity and influence in the dissolution rate. Additionally, it provides the possibility of industrial transposition, being therefore, a technique quite employed [11].

The solubility of the Hydrochlorothiazide (HCTZ) is extremely low; thus, the dissolution rate is the speed limiting step in oral absorption and consequently the bioavailability of this API. Hydrochlorothiazide corresponds chemically to the 6-chloro-3,4-dihydro-2H-1,2,4-sulfonamide benzotiadiazina 7,1,1-dióxido, which presents as a white or almost white odorless crystalline powder with an average weight of 297.7 g mol^{-1} . It is a diuretic drug, widely used as an antihypertensive agent in the form of orally-administered immediate-release tablets [12, 13].

To overcome the low bioavailability and provide a greater diuretic effect, several studies using different types of pharmaceutical technology have been developed to propose a new pharmaceutical form that maximize the actions of HCTZ and simultaneously improve the patient adherence to the treatment, due to the reduced full therapeutic dose of the drug. Thus, Corveleyn and Remon [14] employed the technique of lyophilization with maltodextrin, xanthan gum and PEG 6000; Chadha et al. [15] used multicomponent crystal HCTZ with nicotinic acid (HCTZ-NA) and 2-picolinic acid (Pic-HCTZ); El-Gizawy et al. [16] proposed the formation of co-crystal HCTZ with Aerosil® 200 in the presence of acetone, and Khan et al. [17] used the liquid-solid and solid dispersion techniques with PEG-4000. All these studies confirmed a significant increase in solubility, or even in the API therapeutic activity. Furthermore, some pharmaceutical products containing HCTZ have been patented as an alternative model to increase the dissolution efficiency of the API and increase antihypertensive activity by associating it with other classes of antihypertensive agents [18–20]. Therefore, Chongkai et al. [21] developed and patented (CN103006566A) a sustained release tablet with osmotic pump system containing HCTZ-associated Losartan potassium in the form of solid dispersion (with urea or povidone) or HCTZ as inclusion complex (with hydroxypropyl-beta-cyclodextrin). With this product, the researchers managed to improve the dissolubility of HCTZ and to control speeds of APIs release up to 24 h.

In order to characterize the pharmaceutical product developed, and to evaluate compatibility of the raw materials, various analytical tools can be used, namely: thermal analysis (differential scanning calorimetry—DSC and

thermogravimetry—TG), X-ray powder diffraction (XRPD), Fourier transform infrared spectroscopy (FTIR) and scanning electron microscopy (SEM) [5, 22]. The application of these techniques in an appropriate and integrated manner allows us to evaluate the existence of polymorphism, the interaction between the formulation components, the change in the crystal structure of the API, the size of the particles formed and stability.

In this context, the aim of this study was to characterize solid dispersions of HCTZ obtained with different processing adjuvants, using the DSC, TG, XRPD, FTIR and SEM techniques, and to evaluate the influence of carriers used in the biopharmaceutical performance, by analyzing the efficiency of conventional dissolution mediums.

Experimental

Materials

Hydrochlorothiazide (99.3% purity) was purchased from Gemini (Brazil). Sodium lauryl sulfate (SLS) was purchased from Mapric; polyvinylpyrrolidone K30 (PVP K30) was obtained from All Chemistry; polyethylene glycol 1500 (PEG 1500) and colloidal silicon dioxide Aerosil® 200 (AER) were purchased from Henrifarma.

Control assay: HCTZ-carrier interaction study

HCTZ-carrier control samples were prepared by the physical blend (PB) of HCTZ powder with each carrier (Table 1), without the previous solubilization of HCTZ in the solvent. The mixtures were prepared at a 1:1 (m/m) ratio, manually, using a mortar and pestle with grinding and homogenizing for 10 min. These samples were used to evaluate the effect of each excipient alone in the amorphization process of the API and check the occurrence of interactions between the components.

Obtaining solid dispersion

Solid dispersions (Table 1) were obtained in the ratio 1:1 API/carrier by the solvent method, and spray drying was used as the drying technique. For this purpose, the carrier is first solubilized in 250 mL of ethanol/water (50:50, m/m) and then slowly added to the API, keeping the mixture warm in a magnetic stirrer for 40 min. Finally, 25% of aerosil (m/m), in relation to the total mixture (API + carrier), were added as a drying agent. Therefore, the total solute concentration was 7.5% (m/m). The suspensions were subjected to *spray drying* (SD—Basic Spray Dryer—Lab Plant), with an inlet temperature of 170 °C, an exhaust temperature of 90 °C and a peristaltic pump flow rate of

Table 1 Composition of physical blend and solid dispersions

| Formulation code | Production method | Composition/mass | | | | | Solvent |
|------------------|-------------------|------------------|----------|-----|---------|-----|---|
| | | HCTZ | PEG 1500 | SLS | PVP K30 | AER | |
| HCTZ Crystalline | N/A* | 1 | 0 | 0 | 0 | 0 | N/A |
| PB 1 | Physical blend | 2 | 2 | 0 | 0 | 0 | N/A |
| PB 2 | | 2 | 0 | 2 | 0 | 0 | N/A |
| PB 3 | | 2 | 0 | 0 | 2 | 0 | N/A |
| SD 1 | Spray drying | 8 | 8 | 0 | 0 | 4 | Ethanol in H ₂ O (50:50, m/m) |
| SD 2 | | 8 | 0 | 8 | 0 | 4 | |
| SD 3 | | 8 | 0 | 0 | 8 | 4 | |

* N/A: not applicable

7 mL min⁻¹. The SDs were stored in airtight containers and placed in a desiccator at 25 °C.

Characterization of raw materials and solid dispersions

Differential scanning calorimetry (DSC)

DSC curves were obtained using DSC-60 Shimadzu[®] under a dynamic nitrogen atmosphere with a flow rate of 50 mL min⁻¹. Samples of about 2 mg were weighed and placed in a sealed aluminum sample holder. The analysis was carried out in a temperature range from 25 to 350 °C at a heating rate of 10 °C min⁻¹. The results were analyzed in the OriginPro 8[®] software, to identify thermal events displayed as well as the temperature (T_{peak} and T_{onset}) and ΔH energy (J g⁻¹) involved in these events.

Thermogravimetry (TG)

TG curves were obtained in a PerkinElmer[®] thermobalance (TGA Pyris 1) using alumina crucible. Samples with a mass of approximately 5 mg were subjected to a heating rate of 10 °C min⁻¹ in a temperature range of 25–750 °C under an atmosphere of nitrogen (50 mL min⁻¹). The thermogravimetric curves were analyzed in OriginPro 8[®] software to identify the percentages and initial and final temperatures of mass loss.

Fourier transform infrared spectroscopy (FTIR)

Tablets of the samples were prepared using potassium bromide (KBr) as an inert substance at a ratio of 2:100 API/KBr. The absorption spectra in the infrared region (IR) were obtained on a Prestige 21—Schimadzu IR spectrometer, in the region from 4000 to 400 cm⁻¹. Data were analyzed with OriginPro 8[®].

X-ray powder diffraction (XRPD)

The patterns generated by X-ray diffraction of the samples were recorded on a diffractometer D2 Phaser (Bruker[®] AXS-CuK α , geometry θ – 2θ , voltage 30 kV and 10 mA, step size of 0.02° 2θ – $2^\circ 2\theta$ /min, main slot = 2 mm \times 12 mm and slit receipt = 0.2 mm \times 12 mm, with graphite monochromator). Scans of samples were performed in angular ranges from 5° to 40° (2θ). For a better presentation of the diffraction, X-ray intensities were plotted with OriginPro 8[®].

Scanning electron microscopy (SEM)

Microscopic analysis was performed using a scanning electron microscope (Hitachi TM-1000 model) using acceleration voltage of 15 kV electron beam. Samples were fixed in the sample holder and then metallized. Images were recorded at an increase of 5000 times their original size.

Dissolution study

Dissolution profile

To determine the dissolution profile, 900 mL of hydrochloric acid (HCl) 0.1 M was used as the dissolution medium at a temperature of 37 \pm 0.5 °C in the Nova Ética[®] dissolutor (Model: 299) using the apparatus USP II (paddle) at 50 rpm for 60 min. Aliquots of 5 mL were withdrawn at predetermined intervals (5, 10, 15, 30, 45 and 60 min), filtered through a 0.45- μ m syringe filter, diluted in 0.1 M HCl in the ratio 1:4 and analyzed in the UV spectrophotometer (Schimadzu—Model: UV-1650PC) to 271 nm. The assay was performed in triplicate. The samples were encapsulated using gelatin capsules. The amount of HCTZ used was 50 mg or the concentration equivalent to the dispersions. Data were analyzed with OriginPro 8[®].

Dissolution efficiency (DE)

The dissolution efficiency (DE) was calculated from the values of the area under the curve (AUC) of the dissolution of the HCTZ profile in the time interval (t) using the trapezoidal method [23]. The DE was determined from the ratio of the AUC 0–60 min (AUC 0–60 min) and the total area of the rectangle (ASCTR) defined by the maximum amount (%) dissolved in ordinate and the abscissa ($t = 60$ min). The DE was expressed as a percentage of the area of the rectangle depicting 100% dissolution using Eq. 1.

$$DE = \frac{ASC_{(0-60)}}{ASC_{TR}} \times 100\% \quad (1)$$

Statistical analysis

The results were achieved by analysis of variance (ANOVA), followed by Bonferroni post-test. The results were expressed as means and with significance level of $p < 0.05$.

Results and discussion

Characterization of pharmaceutical ingredients and solid dispersions

Differential scanning calorimetry

Figure 1 illustrates that hydrochlorothiazide showed two events: the first endotherm, attributed to the melting of the HCTZ with a peak temperature of 271.7 °C ($\Delta H_{\text{fusion}} = 240.7 \text{ J g}^{-1}$) and the second exothermic, with a peak temperature of 312.9 °C related to its degradation, as shown in the literature for this API [24, 25]. However, in all physical blends (Fig. 1a), it was observed the disappearance of the melting peak of HCTZ, which can be attributed to the solubilization of the API in the previously melted excipient or in the elastic state (PVP K30), and not necessarily the amorphization of the API.

By analyzing the curves of the solid dispersions SD 1 and SD 3 (Fig. 1b), it was observed that the drying process by nebulization (using aerosil as the drying adjuvant) resulted in the formation of amorphous solid dispersions for these preparations, considering that no thermal events were observed. This was similar to the literature that reported API amorphization of solid dispersions prepared with several classes of active ingredients [26–28]. In general, the SD resulted in amorphization of the API, which in turn influenced the dissolution, bioavailability, stability and other properties thereof [3, 29].

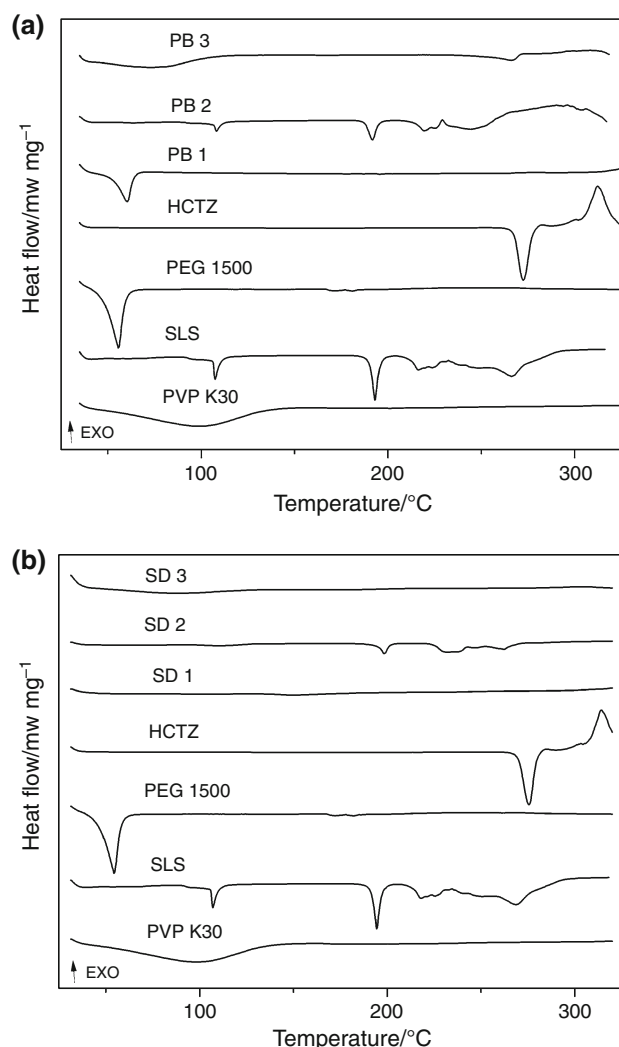


Fig. 1 DSC curves from excipients, HCTZ **a** physical blends, **b** solid dispersions

In the DSC curve of the solid dispersion HCTZ/LSS (SD 2), the disappearance of the melting point of the HCTZ was observed, but a thermal behavior similar to excipient with an endothermic peak at 190.5 °C ($\Delta H_{\text{fusion}} = 16.1 \text{ J g}^{-1}$) was found. This is possibly related to melting of the excipient, although due to an interaction between species, the behavior showed up early, had little intensity and low enthalpy, which suggests partial amorphization of the API.

Thermogravimetry

In Fig. 2, it was observed that the HCTZ showed thermal stability up to 309.7 °C, indicating that the compound is in its anhydrous form. Decomposition of this IFA occurred in three stages (Table 2), the first being the determining step ($T_{\text{onset}} = 309.7 \text{ °C}$, $T_{\text{end}} = 381.6 \text{ °C}$, $\Delta m = 38.1\%$). It was also found that the high-temperature degradation of

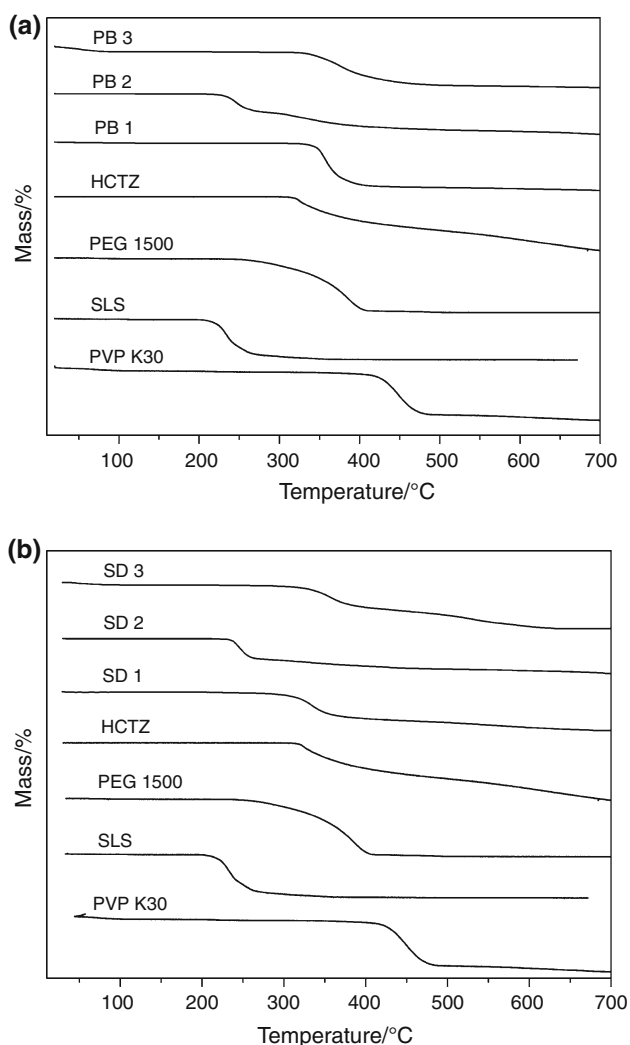


Fig. 2 TG curves from excipients, HCTZ **a** physical blends, **b** solid dispersions

excipients suggested good thermal stability thereof and was safe to use spray drying as the drying method for producing solid dispersions.

Through the profiles of dynamic thermogravimetric curves obtained in nitrogen atmosphere (Fig. 2b) and the values displayed in Table 2, we can conclude that, with the exception of SD 2 ($T_{\text{onset}} = 230.3$ °C), the other dispersions are characterized by thermal decomposition temperatures near the crystalline IFA, indicating that the SD production process retained the thermal stability of HCTZ. This same behavior was reproduced in physical blends (Fig. 2a).

Fourier transform infrared spectroscopy

The FTIR spectrum of HCTZ (Fig. 3) showed a similar profile to that found by Nath and Saria [30] and Padma et al. [31], which were verified characteristic bands

Table 2 Dynamic TG of HCTZ and its SD

| Sample | Decomposition step | T_{onset}^a / °C | T_{end}^a / °C | Δm^b / % |
|--------|--------------------|---------------------------|-------------------------|------------------|
| SD 1 | I | 290.0 | 366.6 | 37.1 |
| | II | 369.0 | 517.3 | 12.1 |
| | III | 518.9 | 682.0 | 11.7 |
| SD 2 | I | 230.3 | 266.6 | 32.7 |
| | II | 268.9 | 743.2 | 29.1 |
| SD 3 | I | 40.7 | 102.6 | 3.8 |
| | II | 300.3 | 386.6 | 32.8 |
| | III | 388.4 | 512.6 | 18.2 |
| | IV | 515.8 | 636.3 | 19.3 |
| HCTZ | I | 309.7 | 381.6 | 38.1 |
| | II | 381.6 | 531.0 | 26.9 |
| | III | 531.0 | 727.6 | 34.8 |

^a T_{onset} / °C and T_{end} / °C refer to the temperatures at which start and end of each step of decomposition

^b Δm % = $\%m_{\text{end}} - \%m_{\text{initial}}$ represents the percentage of mass loss at each step

at 3362, 3265 and 3169 cm^{-1} , which may be attributed to the binding of N–H primary sulfonamides (doublet) and secondary (singlet). The band at wave number 3392 cm^{-1} was attributed to a nitrogen bond of the secondary amine, which is virtually free from hydrogen bonds due to their ability to donate protons. The band in the region 1602 cm^{-1} was attributed to overlapping absorption bands associated with deformations of the C–C bonds and the C=C bonds of the aromatic ring. Those located in 1334, 1319 and 1165 cm^{-1} were associated with the SO_2 group of the sulfonamide, while the band at 1123 cm^{-1} was linked to the heterocyclic ring SO_2 . The FTIR spectra of physical blends PB 2 and PB 3 (Fig. 3a) correspond to the overlapping of the spectra of the API and the excipient alone, which suggests the absence of molecular interactions between the blend components.

The FTIR spectrum of SD 1 (Fig. 3b) and PB 1 (Fig. 3a) showed suppression of the main characteristic bands of HCTZ with the exception of the band at 1602 cm^{-1} (associated with the superposition of the C–N bands and C=C in aromatic ring), which appeared less intense than anticipated. The main characteristic bands of the isolated polymer (PEG 1500) could be verified; however, they were less significant and displaced. According to Fouseris et al. [32], changes to the lower absorption wave numbers indicate the formation of hydrogen bonds.

But the spectrum of SD 2 corresponded to the overlap of API spectra and adjuvant, without significant differences in characteristics bands of the separate components. This suggests the absence of molecular chemical interactions between HCTZ and the LSS, the studied proportions.

In the infrared spectrum of SD 3, it was observed that HCTZ characteristics bands at 3362, 3265 and 3169 cm^{-1} ,

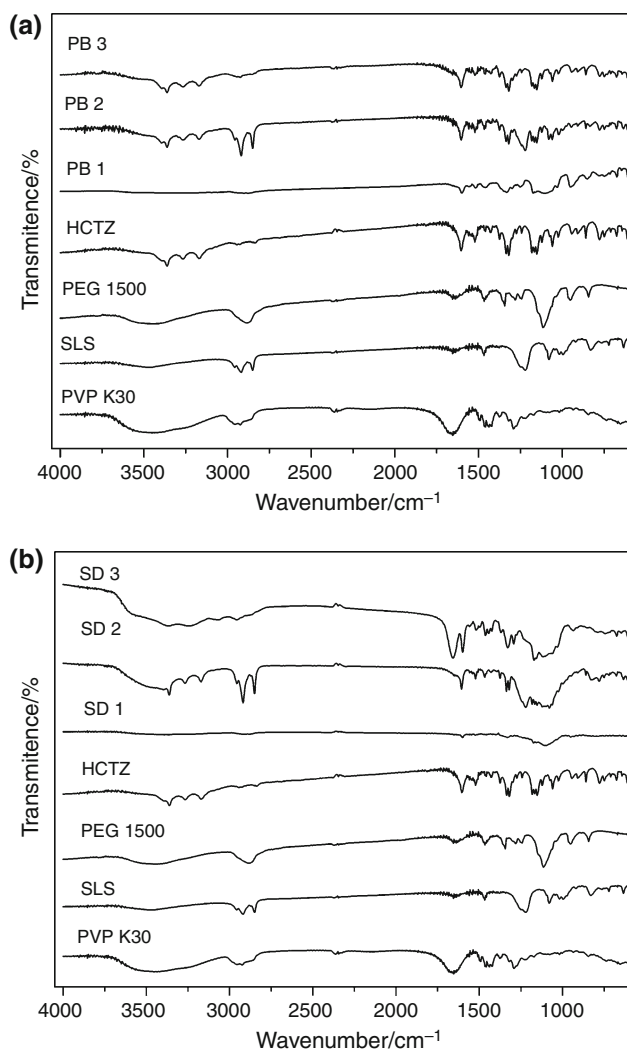


Fig. 3 FTIR spectra from excipients, HCTZ **a** physical blends, **b** solid dispersions

the connection N–H of the sulfonamides was of little significance, extended and displaced to wave numbers 3359, 3235 and 3064 cm⁻¹, respectively. The most important polymer bands (2956 and 1653 cm⁻¹) also remained present in low amounts and displaced (2951 and 1656 cm⁻¹).

Therefore, through the observed results, it is inferred that, with the exception of SD 2, all of the solid dispersions were intermolecular interactions between the polymer and the API, particularly hydrogen bonds, whereas HCTZ is a substance containing polar groups (e.g., –Cl, N–H) which are capable of interacting with other functional groups (e.g., C=O, O–H) present in the polymers and forming bonds such as hydrogen bonds or Van der Waals forces.

X-ray powder diffraction

The Fig. 4 shows the X-ray diffractogram of hydrochlorothiazide, in which a characteristic pattern of

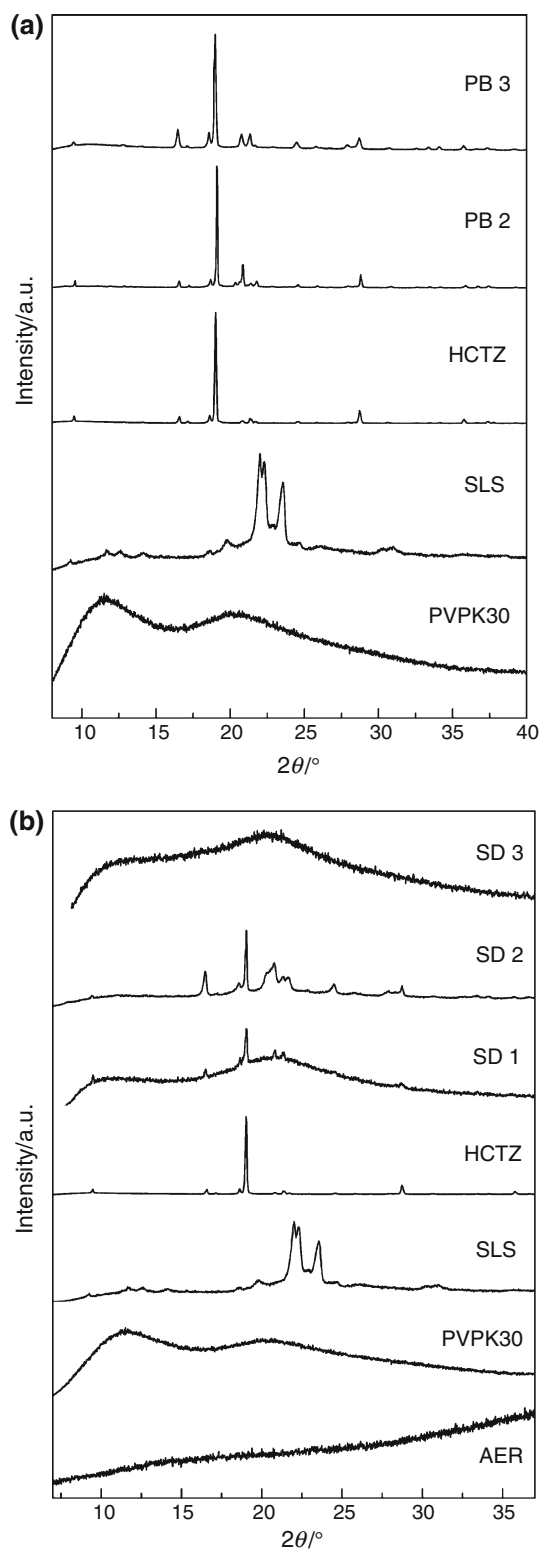


Fig. 4 XRPD patterns from excipients, HCTZ **a** physical blends, **b** solid dispersions

crystalline material with sharp peaks and the most intense reflections at 2θ with values of 16.6°, 19.0° (100%) and 28.7° was observed. Similar diffraction patterns were

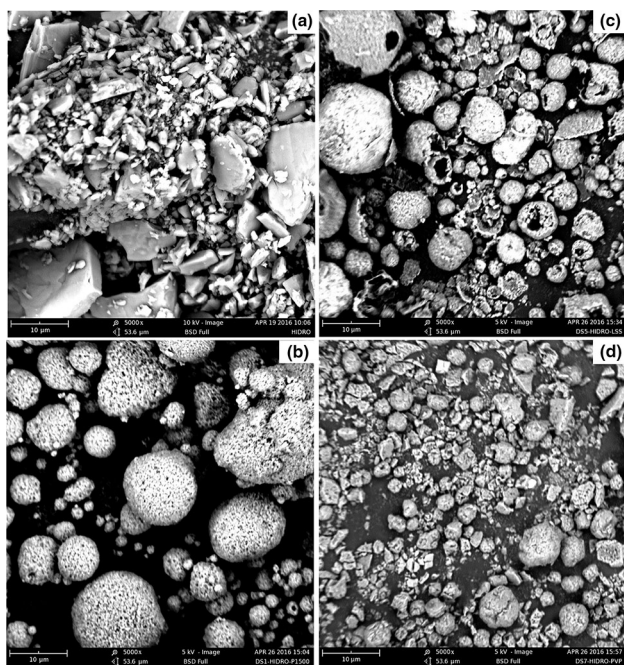


Fig. 5 Photomicrographs of: **a** HCTZ, **b** SD 1, **c** SD 2, **d** SD 3

described by El-Gizawy et al. [16] and Trivedi et al. [33]. The X-ray diffractogram of physical blends (Fig. 4a) revealed the presence of all characteristic peaks of HCTZ, indicating that the crystal structure of the API was not altered in the mixture of raw materials. It was not possible to obtain the diffractogram of PEG 1500 and PB 1 mixture because both of them have no powder characteristic.

The X-ray diffractogram of the SD 3 dispersion (Fig. 4b) showed a characteristic pattern of amorphous material, due to the absence of long-range ordering, confirming what the DSC data suggested. The intermolecular interaction of the type of hydrogen bonding between API: carrier, which was detected in the FTIR spectrum, inhibited the crystallization of the IFA and, consequently, favored the amorphization of the same. According to Veronez et al. [5], the degree of inhibition of crystallization is dependent upon the API/carrier ratio, so a greater inhibition of crystallization is achieved in larger proportions of pharmaceuticals adjuvant.

In the diffractograms from SD 1 and SD 2 (Fig. 4b) dispersions, it was verified the presence of wider peaks at 2θ values similar to the HCTZ. However, the samples showed a high amorphization degree, confirming the information previously obtained by DSC technique.

Scanning electron microscopy

The scanning electron microscope allows us to identify the morphology and chemical elements of solid samples [34]. In the photomicrograph of HCTZ (Fig. 5a), crystals

with a smooth, lamellar shape, with jagged edges of varying sizes, were observed.

In the solid dispersion obtained by spray drying (Fig. 5b–d), the microparticles presented topographically with a tendency to sphericity, and the SD1 dispersion showed a high porosity on its surface. The presence of hollow spheres (Fig. 5c) was also noted. This spherical shape can promote increase in surface area and encourage greater solubility of the product, because according to Ansel et al. [35], the morphology of identification suggested the API's behavior in relation to its dissolution rate and the rate and extent of absorption in vivo.

Furthermore, according to Vieira et al. [36], crystal structures in the form of irregular cubes or spheres, when compared with those needles of crystalline habit, have better flow properties, which facilitates its manipulation for the development of solid dosage forms.

Dissolution study

Dissolution is used to check the quality of the product and the bioavailability of the API. This helps in the choice of excipients, in the development of the manufacturing process, assists post-registration changes and promotes studies in vitro–in vivo [37].

Figure 6 shows that the API crystalline had dissolved 54% in 60 min (Table 3). However, according to the US Pharmacopeia [38], in dissolution test preparations containing HCTZ, no less than 60% of the drug must dissolve within 60 min. In the physical blends (Fig. 6a), it was observed that there was no dissolution increase in the API, statistically significant.

Comparing the dissolution profile of SDs with isolating HCTZ (Fig. 6b), SD 1 and SD 3 dispersions showed a dissolution rate greater than the API, meaning the process for SD production was extremely effective in increasing API dissolution low solubility. According to Veronez et al. [5], amorphous forms of API often exhibit desirable physicochemical properties, such as higher dissolution rates and improved solubility, compared to their crystalline counterparts.

Amorphous particles have a rapid dissolution rate because they are highly soluble. They have high energy and higher molecular mobility when compared to particles of defined form (crystalline) that exhibit a lower dissolution rate [34].

The DE consists of the integral comparative evaluation of the area under the curve (AUC) of the dissolution profile compared to the area represented by the total test time. The use of the dissolution efficiency for comparison between formulations has been advocated by several authors, since bioavailability is also determined by calculating the AUC [39].

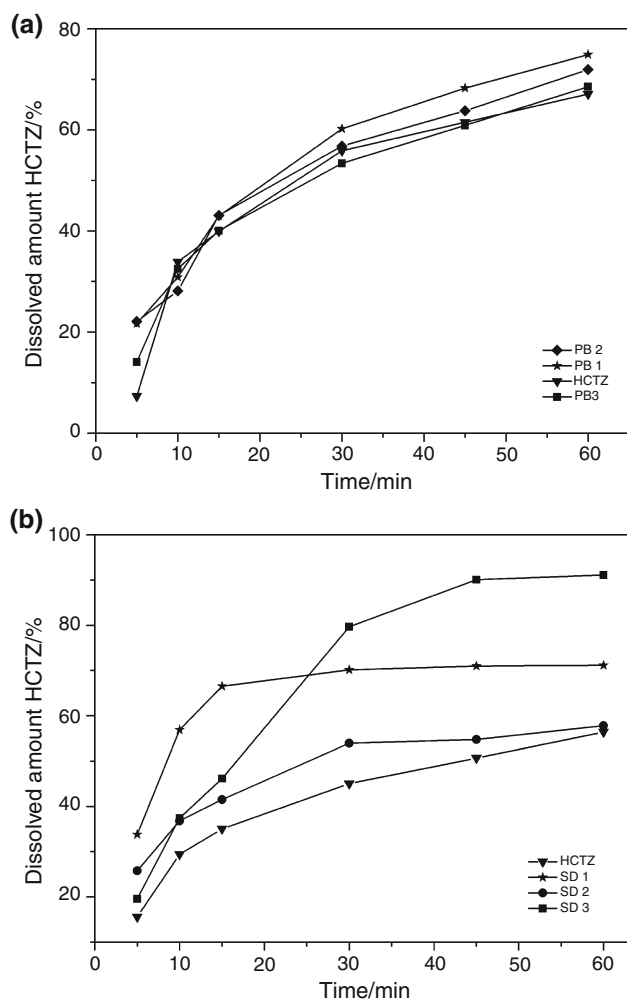


Fig. 6 Dissolution profile of HCTZ and solid dispersions

Table 3 Dissolved amount of API and dissolution efficiency

| Sample | Dissolution/ % | DE/ % |
|------------------|----------------|---------|
| HCTZ crystalline | 54.0 | 39.3 |
| PB 1 | 71.4 | 51.1 |
| PB 2 | 63.8 | 49.5 |
| PB 3 | 55.0 | 40.0 |
| SD 1 | 75.6* | 66.8* |
| SD 2 | 58.7 | 46.3 |
| SD 3 | 98.4*** | 74.9*** |

Data expressed as mean ($n = 3$). * $p < 0.05$; ** $p < 0.01$; *** $p < 0.001$ compared with HCTZ. The absence of an asterisk shows the data were not significant

Comparing the values of the DE of the HCTZ crystalline with the SD (Table 3) revealed that SD 1 and SD 3 increased the AUC of the dissolution profile of isolated HCTZ, particularly SD 3 (HCTZ/PVP K30), which showed a DE of approximately 75%. This represents a 90% increase in dissolution in relation to HCTZ.

The solid dispersion with the water dispersible carrier is currently one of the strategies most commonly used to overcome the limitations of solubility in water. The solid dispersion method can be used to improve the dissolution characteristics of the hydrophobic API and increase its bioavailability. The distribution of the API in the carrier, along with increased wettability promoted by the carrier, can enhance solubility and dissolution rate [27].

Conclusions

The DSC and XRPD techniques showed that the nebulization process formed amorphous solid dispersions, and that according to FTIR data, the amorphization of the HCTZ was due to intermolecular interactions of the type of hydrogen bonds between the API and the carrier (specifically PEG 1500 and PVP K30). The thermogravimetric study already demonstrated that the thermal decomposition of the dispersion occurred at temperatures near the crystalline API, with the exception of SD 2, indicating that the manufacturing process maintained the stability of HCTZ.

The SEM showed that the spray-drying technique originated microparticles with a tendency to sphericity. Acquired morphology associated with amorphization contributed to the increased dissolution rate and DE of dispersions. However, SD 3 (HCTZ/PVP K30) presented the best HCTZ dissolution increase, which certainly contributed to greater bioavailability of this API. In this sense, one can propose a new pharmaceutical formulation using the SD in order to enhance the actions of HCTZ.

It is concluded, therefore, that the analytical techniques described here were of fundamental importance to the characterization of pharmaceutical product developed—including its morphology, thermal stability, prediction of the crystalline form of the solid phase, intermolecular interactions between the API and the carrier, and presumption of oral API bioavailability.

Acknowledgements We thank Coordination of Improvement of Higher Level Personnel (CAPES) for funding this work and to Laboratory of Evaluation and Development of Northeastern Biomaterials (CERTBIO) of the Federal University of Campina Grande and to Materials Engineering Laboratory of the Federal University of Paraíba by analysis provided.

References

- Alves LDS, Lyra MAM, Rolim LA, Presmich GMA, Rolim-Neto PJ. Avanços, propriedades e aplicações de dispersões sólidas no desenvolvimento de formas farmacêuticas sólidas. *Rev Ciênc Farm Básica Apl.* 2012;33:17–25.

2. Truong DH, Tran TH, Ramasamy T, Choi JY, Choi H-G, Yong CS, Kim JO. Preparation and characterization of solid dispersion using a novel amphiphilic copolymer to enhance dissolution and oral bioavailability of sorafenib. *Powder Technol.* 2015;283:260–5.
3. Bikiaris D, Papageorgiou GZ, Stergiou A, Pavlidou E, Karavas E, Kanaze F, Georgarakis M. Physicochemical studies on solid dispersions of poorly water-soluble drugs evaluation of capabilities and limitations of thermal analysis techniques. *Thermochim Acta.* 2005;439:58–67.
4. Vo CL-N, Park C, Lee B-J. Current trends and future perspectives of solid dispersions containing poorly water-soluble drugs. *Eur J Pharm Biopharm.* 2013;85:799–813.
5. Veronez IP, Daniel JSP, Júnior CEC, Garcia JS, Trevisan MG. Development, characterization, and stability studies of ethinyl estradiol solid dispersion. *J Therm Anal Calorim.* 2015;120:573–81.
6. Janssens S, de Armas HN, D'Autry W, Van Schepdael A, Van den Mooter G. Characterization of ternary solid dispersions of Itraconazole in polyethylene glycol 6000/polyvidone-vinylacetate 64 blends. *Eur J Pharm Biopharm.* 2008;69:1114–20.
7. Savjani KT, Gajjar AK, Savjani JK. Drug solubility: importance and enhancement techniques. *Int Sch Res Netw.* 2012;. doi:10.5402/2012/195727.
8. Sethia S, Squillante E. Solid dispersion of carbamazepine in PVP K30 by conventional solvent evaporation and supercritical methods. *Int J Pharm.* 2004;272:1–10.
9. Mogal SA, Gurjar PN, Yamgar DS, Kamod AC. Solid dispersion technique for improving solubility of some poorly soluble drugs. *Der Pharm Lett.* 2012;4:1574–86.
10. Kaur P, Singh SK, Garg V, Gulati M, Vaidya Y. Optimization of spray drying process for formulation of solid dispersion containing polypeptide-k powder through quality by design approach. *Powder Technol.* 2015;284:1–11.
11. Chauhan B, Shimpi S, Paradkar A. Preparation and characterization of etoricoxib solid dispersions using lipid carriers by spray drying technique. *AAPS Pharm Sci Tech.* 2005;6:E405–12.
12. British pharmacopoeia. The stationary office: pharmacopoeia Commission British. Pharmabooks Publisher. 2015; ISBN 10 0113229879.
13. Brunton LL, Chabner BA, Knollmann BC. Goodman and Gilman: as bases Farmacológicas da Terapêutica. 12th ed. Rio de Janeiro: McGraw-Hill; 2012.
14. Corveleyn S, Remon JP. Bioavailability of hydrochlorothiazide: conventional versus freeze-dried tablets. *Int J Pharm.* 1998;173:149–55.
15. Chadha R, Bhandari S, Khullar S, Mandal SK, Jain DV. Characterization and evaluation of multi-component crystals of hydrochlorothiazide. *Pharm Res.* 2014;31:2479–89.
16. El-Gizawy SA, Osman MA, Arafa MF, El Maghraby GM. Aerosil as a novel co-crystal co-former for improving the dissolution rate of hydrochlorothiazide. *Int J Pharm.* 2015;478:773–8.
17. Khan A, Iqbal Z, Shah Y, Ahmad L, Ullah Z, Ullah A. Enhancement of dissolution rate of class II drugs (hydrochlorothiazide); a comparative study of the two novel approaches; solid dispersion and liqui-solid techniques. *Saudi Pharm J.* 2015;23:650–7.
18. Fengming L. Candesartan hydrochlorothiazide dispersible tablets and the preparing method thereof. CN101062038A; 2007.
19. Roller N. A Losartan potassium hydrochlorothiazide pharmaceutical composition liposome solid preparation. CN101797230A; 2010.
20. Minggui Y. Lisinopril and hydrochlorothiazide pharmaceutical composition liposome solid preparation. CN102166208B; 2011.
21. Chongkai G, Huiqiu H, Ning L, Jie J. Osmotic pump controlled release tablet of losartan potassium and hydrochlorothiazide solid dispersion or inclusion compound. CN103006566 A; 2013.
22. Górnaiak A, Gajda M, Pluta J, Czapor-Irzabek H, Karolewicz B. Thermal, spectroscopic and dissolution studies of lovastatin solid dispersions with acetylsalicylic acid. *J Therm Anal Calorim.* 2016;. doi:10.1007/s10973-016-5279-z.
23. Khan KA, Rhodes CT. The concept of dissolution efficiency. *J Pharm Pharmacol.* 1975;27:48–9.
24. Oliveira MA, Yoshida MI, Silva DCGM. Quality evaluation of pharmaceutical formulations containing hydrochlorothiazide. *Molecules.* 2014;19:16824–36.
25. Brazilian pharmacopoeia. Farmacopéia Brasileira. 5th ed. Brasília: Agência Nacional de Vigilância Sanitária; 2010. p. 546.
26. Mashru RC, Sutariya VB, Sankalia MG, Yagnakumar P. Characterization of solid dispersions of rofecoxib using differential scanning calorimeter. *J Therm Anal Calorim.* 2005;82:167–70.
27. Yu M, Sun L, Li W, Lan Z, Li B, Tan L, Li M, Yang X. Investigation of structure and dissolution properties of a solid dispersion of lansoprazole in polyvinylpyrrolidone. *J Mol Struct.* 2011;1005:70–7.
28. Shi C, Tong Q, Fang J, Wang C, Wu J, Wang W. Preparation, characterization and in vivo studies of amorphous solid dispersion of berberine with hydrogenated phosphatidylcholine. *Eur J Pharm Sci.* 2015;74:11–7.
29. LaFontaine JS, Prasad LK, Brough C, Miller DA, McGinity JW, Williams RO III. Thermal processing of PVP- and HPMC-based amorphous solid dispersions. *AAPS Pharm Sci Tech.* 2016;17:120–32.
30. Nath MR, Saria M. Synthesis: isolation and characterization of hydrochlorothiazide dimer impurity. *Int J Pharm Pharm Sci.* 2013;5:867–71.
31. Padma PS, Rajendran NN, Lakshmi PK, Umadevi SK, Vajjayanthi V, Kausalya J, Ravichandran V. A novel captopril hydrochlorothiazide solid dispersion. *Int J Pharm Pharm Sci.* 2010;2:30–2.
32. Fouteris E, Tarantili PA, Karavas E, Bikiaris D. Poly(vinyl pyrrolidone)–poloxamer-188 solid dispersions prepared by hot melt extrusion: thermal properties and release behavior. *J Therm Anal Calorim.* 2013;113:1037–47.
33. Trivedi RV, Admane PS, Taksande JB, Mahore JG, Umekar MJ. Solubility enhancement studies of hydrochlorothiazide by preparing solid dispersions using losartan potassium and urea by different methods. *Der Pharm Lett.* 2011;3:8–17.
34. Chieng N, Rades T, Aaltonen J. An overview of recent studies on the analysis of pharmaceutical polymorphs. *J Pharm Biomed Anal.* 2011;55:618–44.
35. Ansel HC, Popovich NG, Allen LV. Formas Farmacêuticas and Sistemas de Liberação de Fármacos. 8th ed. São Paulo: Artmed; 2007.
36. Vieira ACQM, Marques GS, Melo CM, Silva KER, Rolim LA, Lima MCA, Galdino SL, Pitta IR, Rolim-Neto PJ. Physical–chemical characterization of new anti-inflammatory agent (LPSF/GQ-130) and evaluation of its thermal compatibility with pharmaceutical excipients. *J Therm Anal Calorim.* 2014;115:2339–49.
37. Storpirtis S, Gonçalves JE, Chiann C, Gai MN. *Biofarmacotécnica.* 2^a ed. Rio de Janeiro: Editora Guanabara Koogan; 2011.
38. United States Pharmacopoeia and National Formulary USP 29-NF 24. Pharmacopoeial Convention, Rockville; 2010.
39. Mahle F, Goelzer F, Adriano J, Felipe M, Vier N, Carli RBG, Rosa T, Couto AG, Lucinda-Silva RM. Avaliação do perfil de dissolução de comprimidos de hidroclorotiazida comercializados no Brasil. *Rev Ciênc Farm Básica Apl.* 2007;28:265–71.